CHEMISTRY
A EUROPEAN JOURNAL

DOI: 10.1002/chem.201002588

The Role of Surface and Subsurface Point Defects for Chemical Model Studies on TiO_2: A First-Principles Theoretical Study of Formaldehyde Bonding on Rutile TiO_2(110)

Jan Haubrich,[a] Efthimios Kaxiras,[b, c] and Cynthia M. Friend*[a, b]

Abstract: We report a systematic investigation of the effects of different surface and subsurface point defects on the adsorption of formaldehyde on rutile TiO_2(110) surfaces using density functional theory (DFT). All point defects investigated—including surface bridging oxygen vacancies, titanium interstitials, and subsurface oxygen vacancies—stabilize the adsorption significantly by up to 56 kJ mol^{-1} at a coverage of 0.1 monolayer (ML). The stabilization is due to a decrease of the coordination (covalent saturation) of the surface Ti adsorption sites adjacent to the defects, which leads to a stronger molecule–surface interaction. This change in the Ti is caused by the removal of a neighboring atom (oxygen vacancies) or substantial lattice relaxations induced by the subsurface defects. On the stoichiometric reference surface, the most stable adsorption geometry of formaldehyde is a tilted η^2-dioxymethylene (with an adsorption energy $E_{ads} = -125$ kJ mol^{-1}), in which a bond forms to a nearby bridging O atom and the carbonyl-O atom in the formaldehyde binds to a Ti atom in the adjacent fivefold coordinated lattice site. The η^1-top configuration on five-coordinate Ti^{4+} is much less favorable ($E_{ads} = -69$ kJ mol^{-1}). The largest stabilization is exerted by subsurface Ti interstitials between the first and second layers. These defects stabilize the η^2-dioxymethylene structure by nearly 40 kJ mol^{-1} to an adsorption energy of -164 kJ mol^{-1}. Contrary to popular belief, adsorption in a bridging oxygen vacancy ($E_{ads} = -86$ kJ mol^{-1}) is much less favorable for formaldehyde compared to the η^2- dioxymethylene structures. From these results we conclude that formaldehyde will bind in the η^2-dioxymethylene structure on the stoichiometric surface as well as in the presence of Ti interstitials and bridging oxygen vacancies. In the light of these substantial effects, we conclude that it is essential to include all the types of point defects present in typical, reduced rutile samples used for model studies, at realistic concentrations to obtain correct adsorption sites, structures, energetic, and chemi-physical properties.

Keywords: density functional calculations · point defects · subsurface defects · surface chemistry · surface defects · titanium dioxide

Introduction

The rutile TiO_2(110) surface is one of the most-widely investigated models of reducible oxides surfaces.[1–5] Titania is an important material for catalysis and photocatalysis, rendering it a key material to investigate. However, the characterization of titania represents a great challenge. Defects—shear planes, interstitials, surface and bulk oxygen vacancies—lend titania surfaces their interesting chemical[1–3,6] and physical[1,3,6,7] properties; however, they complicate experimental and theoretical characterization. The types of defects present in a titania sample depend strongly on the environment, the sample, and its "experimental history".[1,8,9] Even under atmospheric conditions, significant amounts of approximately 0.5 % bulk oxygen vacancies have been reported.[10]

Point defects are crucial in governing the chemical properties of titania surfaces[1,2] because of their potential to stabilize the binding of surface species and act as electron donors and oxygen acceptors in reductive processes. Ti interstitials in the subsurface region stabilize, for example, the molecular adsorption for O_2 on Ti^{4+} sites.[11 12] Once sufficient thermal energy is available, the oxygen dissociates, and the Ti interstitials (5–6 % ML[11]) are drawn to the surface, forming new "TiO_2" clusters.[11,13] Surface oxygen vacancies stabilize the adsorption of as many as three O_2 molecules on adjacent sites at low temperatures.[14] The dissociation of O_2 in a bridging oxygen vacancy induced by annealing to approximately 150 K heals the defect[11,14–17] and leaves an O-adatom on an adjacent five-coordinate Ti^{4+} site behind.[11,14–16,18,19] Adsorption in surface oxygen vacancies is generally also preferred by other oxygenated molecules such as alcohols[1,2, 20–22] or water,[1,2,11,21,23–26] which leads to dissociative channels forming a bridging hydroxyl or an alkoxy in the and a capping bridging hydroxyl from the O–H dissociation.

[a] Dr. J. Haubrich, Prof. C. M. Friend
Department of Chemistry and Chemical Biology
Harvard University, Cambridge, MA, 02138 (USA)
E-mail: cfriend@deas.harvard.edu

[b] Prof. E. Kaxiras, Prof. C. M. Friend
School of Engineering and Applied Sciences
Harvard University, Cambridge, MA, 02138 (USA)

[c] Prof. E. Kaxiras
Department of Physics
Harvard University, Cambridge, MA, 02139 (USA)

A variety of surface and subsurface point defects are presently being considered to be formed in titania by reduction procedures, for example with hydrogen, as well as typical sample preparation methods under vacuum conditions.[1–5] Bulk oxygen vacancies are created by annealing titania to temperatures above 800 K in vacuum[1,27–30] leading to paramagnetic behavior.[1 9,27,30,32] UV[33,34] and IR spectroscopies[35] suggested that bulk oxygen vacancies lead to defect states in the band gap around 0.7 to 1.2 eV below the conduction band (CB), which have been correlated with theoretical computations of density of states (DOS) using non-time dependent density functional theory (DFT).[5,10,36–38] The excess electrons of the defect are transferred to adjacent Ti^{4+} lattice ions, transforming them into reduced "Ti^{3+}" species.[10,36]

Close to the surface, two different types of oxygen vacancies are possible: oxygen vacancies below five-coordinate Ti ions, and those below bridging-oxygen-row Ti ions. Although energetically much less favorable than surface oxygen vacancies,[39] their presence has been implied from scanning tunneling microscopy and spectroscopy (STM/STS) experiments.[1,15,40]

Surface oxygen vacancies can be created similarly by annealing, reduction or bombardment of the surface with electrons or inert gases.[1,11,11, 16, 24, 28, 30, 35, 41–43] Typical surface bridging oxygen vacancy concentrations obtained for samples prepared under ultrahigh vacuum conditions are in the range of approximately 7–15 %.[1, 11, 26, 43–45] They lead to similar band-gap states bulk oxygen vacancies,[14, 28, 40, 41, 46] which is supported from theoretical studies that also found spin-polarized ground states.[19, 37, 47–50] The localization of the excess charge left due to the unsaturated valence of the Ti atoms at the oxygen vacancies is highly controversial and complicated by temperature effects. Resonant photoelectron diffraction (RPD)[51] and STM/STS[40] experiments performed at room temperature suggest that the excess electrons are delocalized over several Ti lattice sites, which is consistent with DFT–GGA (generalized gradient approximation) cluster calculations by Bredow and Pacchioni.[47] Electronic structure calculations excluding temperature effects ("0 K"), on the contrary, performed by Morgan and Watson[50] using a different exchange-correlation functional (PBE+U) found a strong localization and a polaronic distortion. A recent study on anatase showed a similar localization with the PBE+U (for a sufficiently large ad-hoc parameter U) and the hybrid functional B3LYP, but also found delocalized states only slightly higher in energy.[52]

Titanium interstitials are mobile in the lattice and facilitate the "bulk-assisted" reoxidation of titania above about 700 K by diffusion into the bulk.[29,42] Ti interstitials are also proposed to account for band-gap states at approximately 0.8 eV below CB observed spectroscopically and in paramagnetic response,[9, 11, 31, 33, 53] which renders their experimental differentiation from oxygen vacancies problematic. Jenkins and Murphy,[30] for example, proposed that the majority of Ti^{3+} ESR bulk signal stems from O vacancies rather than Ti interstitials. Aono and Hasiguti[31] showed that Ti interstitials have a formal charge state of +III and retain a single unpaired electron ($S=1/2$), thus donating excess electrons to the surrounding lattice. Careful RPD experiments by Krüger et al.[51] also indicate an electron delocalization over adjacent Ti lattice ions similar to the behavior observed for surface oxygen vacancies. Although the "apparent Ti^{3+}" charge state and electron transfer is reproduced in recent DFT-GGA and B3LYP studies, a paramagnetic triplet ($S=1$) ground state with donor levels at 1.1–1.8 eV below CB has been found.[53] The disagreement in the spin state may be attributed to the formation of Ti_2 pairs at higher reduction states.[31]

Herein, we report a systematic investigation of the effect surface and subsurface vacancies on the bonding of formaldehyde to TiO_2(110) as a prototype for aldehyde binding. All adsorption structures considered are stabilized by subsurface vacancies. These results are different than the commonly-held view that oxygenates, including aldehydes and ketones, preferentially bind in bridging oxygen vacancies.[24, 54, 55] The most stable configuration of formaldehyde is a η^2-dioxymethylene structure, in agreement with recent work by others,[56] but at odds with the more common proposal of an η^1-structure with the oxygen bound to a five-coordinate Ti^{4+} site.[57–59] Recently, a structure similar to paraformaldehyde was proposed, though, based on vibrational measurements.[55] The η^2-dioxymethylene structure remains the most favorable adsorption form in the presence of subsurface Ti interstitials and/or surface oxygen vacancies.

These results are discussed in the context of chemical reactivity. Aldehydes readily undergo reductive coupling to olefins requiring loss of oxygen to TiO_2(110).[24, 55, 57, 59] Although oxygen vacancies had been proposed as these coupling sites,[24, 55] recent experiments point to Ti interstitials as the main active point defect for reductive coupling.[57,60]

Results and Discussion

I. Stoichiometric TiO_2(110): Two configurations with very similar energies were identified for an η^1-top geometry, in which the O of the $H_2C{=}O$ is bound to a five-coordinate Ti ion ("Ti_{5c}") on a stoichiometric TiO_2(110) slab (Table 1;

Table 1. Adsorption energies of the formaldehyde configurations on the stoichiometric and defective surface slabs [kJ mol^{-1}].

Binding configuration/ adsorption energy [kJ mol^{-1}]	η^1-top on Ti_{5c}	η^2-dioxymethylene Ti_{5c}/O_{br}	η^2 in O_{br}–V_O	η^2-dioxymethylene in O_{br}–V_O
stoichiometric TiO_2 surface	−69	−125	–	–
TiO_2/O_{br} vacancy	−66	–	−86	−95
I_{Ti} in <110> channel	−90	−164	–	–
I_{Ti} between two channels	−82	−129	–	–
TiO_2/sub-Ti_{5c} V_O	−135	–	–	–
TiO_2/sub-O_{br} V_O	−63	–	–	–

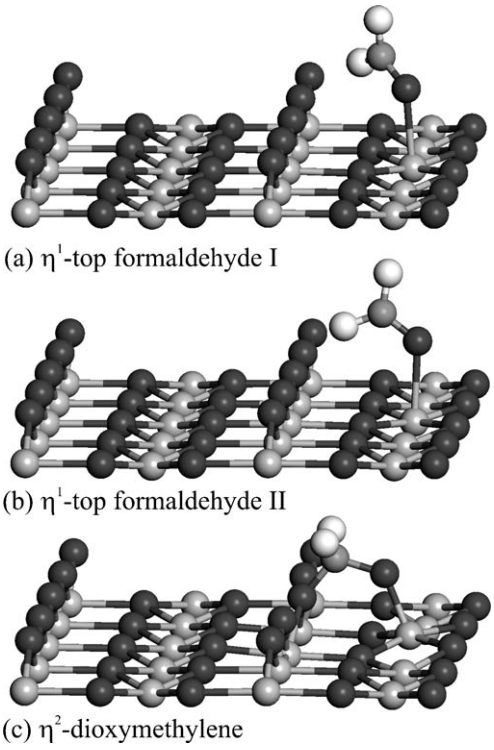

Figure 1. Optimized adsorption geometries of formaldehyde on a stoichiometric TiO_2(110) (a, b and c). For clarity only the surface layer of the 5×2 supercells is shown. Black spheres represent O atoms, gray Ti, dark gray C, and white H.

Figure 1). These calculations were for a low coverage of formaldehyde, 0.1 monolayer (ML), for which interactions between molecules are negligible.

The two configurations differ in the orientation of the vertical molecular plane with respect to the unit cell vectors. One η^1-top configuration, in which the CH_2 group points diagonally to the bridging oxygen rows in the [001] direction (Figure 1a), has a weak a C–H→O_{br} hydrogen bridge bond (bond length 274 pm) and an adsorption energy of $-69\ kJ\,mol^{-1}$. The optimized Ti–O bond length is very long at 223 pm (Table 2) in comparison to the Ti–O lattice bonds on the clean surface,[61] and the C=O bond length of the adsorbed molecule is close to the optimized gas-phase value (121 pm). A second stable η^1-top configuration ($E_{ads}=-66\ kJ\,mol^{-1}$; Figure 1b), in which the CH_2 group is rotated at right angles to the closest bridging oxygen shows very similar structural parameters.

The most stable adsorption configuration of formaldehyde on the stoichiometric rutile (110) surface at low coverages is an η^2-dioxymethylene structure (Figure 1c) with an adsorption energy of $-125\ kJ\,mol^{-1}$ (Table 1). This structure was previously proposed on TiO_2(001) to form by nucleophilic attack of a lattice oxygen on the η^1-top structures, and undergo a subsequent Cannizarro type disproportion to methoxy and formate.[56] Analogously, Henderson and Zehr[58,59] proposed the formation of acetone–oxygen and acetaldehyde–oxygen complexes from addition of oxygen adatoms.

Table 2. Optimized bond lengths in pm and harmonic vibrational frequencies in cm^{-1} for η^1-top formaldehyde configurations on the stoichiometric, subsurface V_O- or I_{Ti}-containing slabs. The outward relaxation is calculated relative to the position in the clean slab with point defect.

Slab	Distance [pm]			Vibrational frequencies [cm^{-1}]	
	$r(Ti_{5c}–O)$	$r(C–O)$	Ti_{5c} outward relaxation	ν(C=O)	$\nu(Ti_{5c}–O)$[a]
stoichiometric	223	123	11	1694	275
sub-Ti_{5c} V_O	196	126	77	1510	335
I_{Ti} in <110> channel	213	123	15	1640	283
I_{Ti} between two <110> channels	216	123	16	1658	286

[a] The $\nu(Ti_{5c}–O)$ modes show strong coupling to δ(H-C-O) modes, which represent the leading component of a normal mode computed around 270 cm^{-1} for these structures.

According to the bond lengths, this structure resembles a geminal diolate with one oxygen atom binding to a Ti_{5c} site ($r(Ti_{5c}–O)=183$ pm, see Table 3), and the second one being an adjacent bridging oxygen atom that attacked the carbonyl carbon atom ($r(Ti_{6c}–O_{br})=206$ pm). In contrast to the η^1-top configurations, the Ti–O bond lengths for this configuration are much shorter, but slightly longer than lattice Ti–O bond lengths (185 pm), and both C=O bond lengths (142 pm) are substantially elongated compared to those in the gas phase.

Table 3. Optimized bond lengths in pm for η^2-dioxymethylene formaldehyde configurations binding to a Ti_{5c} site and a bridging oxygen on the stoichiometric and subsurface I_{Ti} containing slabs. The outward relaxation is calculated relative to the position in the clean slab with point defect.

Distance [pm]/ slab	$r(Ti_{5c}–O)$	$r(C–O)$	Ti_{5c} outward relaxation	$r(Ti_{6c}–O_{br})$	$r(C–O_{br})$
stoichiometric	183	142	42	206	142
I_{Ti} in <110> channel	182	143	66	208	141
I_{Ti} between two <110> channels	183	142	70	198/218	143

The bonding in the η^2 configuration has covalent character, in contrast to the primarily electrostatic character of the η^1-top configurations as can be seen from comparison of the density of states (DOS) projected on the bonding C, O, and Ti atoms (Figure 2). Clearly, the DOS projections on the binding atoms of the η^1-top configuration (Figure 2b) have strong similarities to the bonding MOs of gas-phase formaldehyde (Figure 2a). Although all levels are shifted to lower energies away from the vacuum level (or Fermi energy, respectively), the 6σ level appears to be perturbed slightly more. This MO, which in the gas phase corresponds to a linear combination primarily of the axial $2p_y$ components of C and O, is suitable in symmetry to contribute to a very

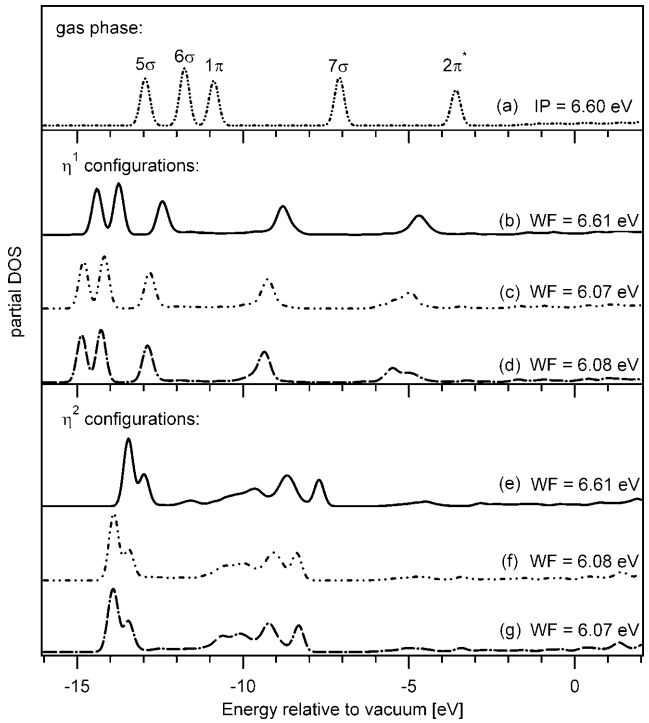

Figure 2. Density of states (DOS) projected on the C, O, and H atoms of formaldehyde in the vacuum between two slabs (gas phase, (a)), and respective η^1 (b–d) and η^2 (e–g) binding configurations on the stoichiometric slab (b and e), with the I_{Ti} in a <110> channel (c and f), and in between two <110> channels (d and g). Workfunctions (WF) are given in eV.

weak covalent interaction with the out-of-plane Ti states such as d_{z^2}. In contrast to the binding of the η^1-top configurations, the resulting "bands" of η^2-adsorbed molecules on stoichiometric TiO_2 (Figure 2e) indicate that new orbitals have been formed with the valence s, p, and, importantly, d states of the bonding Ti_{5c} site and the states of the incorporated bridging oxygen.

The low activation barrier to form the η^2-dioxymethylene structure from the diagonal η^1-top adsorption configuration of 7 kJ mol^{-1} (obtained using the climbing nudged elastic band method) implies that the latter structure can easily convert into the dioxymethylene either during or after adsorption. In the transition state of the pathway, which corresponds mostly to a flipping motion of the CH_2 group over to the nearest bridging oxygen, two C–O bond lengths to the bridging oxygen and the aldehydic oxygen atom are very asymmetric at 228 pm and 125 pm.

II. Bonding to defective surfaces with subsurface Ti interstitials: Subsurface Ti interstitials ("I_{Ti}") stabilize the bonding of formaldehyde substantially by up to 39 kJ mol^{-1} with respect to stoichiometric TiO_2(110) and lead to the most stable adsorption configurations on any of the surfaces considered. To obtain an upper bound of the stabilization effects, we considered an I_{Ti} right below binding sites between the first and second trilayer. A recent DFT study proposed the most stable binding site of an interstitial in a five trilayer slab to be between the second and third trilayers (more stable by up to 20 kJ mol^{-1}),[11] but found the diffusion barrier to the surface to be as low as 72 kJ mol^{-1} in the presence of a surface O_2 molecule, which indicates that their movement may be facile around and above room temperature.

Two different binding sites of Ti interstitials below the surface have been obtained and both are energetically very similar in the clean slab (the second one lower by only 2 kJ mol^{-1}). The tested positions are I) in a vertical <110> channel (Figure 3a and 3b), and II) between two such adjacent <110> channels (Figure 3c and 3d). We found the optimized solutions for spin-polarized triplet states of those I_{Ti} at 5 and 1 kJ mol^{-1} higher in energy than the singlet states, respectively.

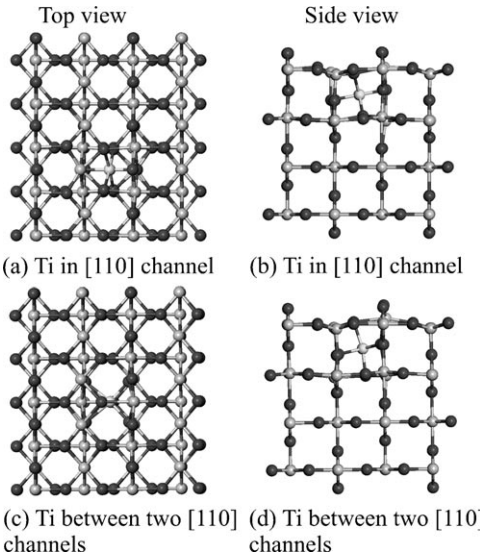

Figure 3. Optimized geometries of the two I_{Ti} binding sites obtained in between the first and second trilayer. a) Top and b) side views of the I_{Ti} (highlighted in yellow) bonded in a [110] channel; c) and d) the geometries for the I_{Ti} bonded between two [110] channels.

In these structures, the I_{Ti} induces strong changes in the lattice, particularly around the adjacent Ti_{5c} adsorption sites at the surface. The Ti_{5c} atom is relaxed outward by effectively 20 pm in both cases, with the bonds to the underlying lattice oxygen elongated from 183 pm to 193 pm (I_{Ti} type I) and 190 pm (I_{Ti} type II), and the bonds of the latter oxygen to its bulk Ti_{6c} neighbors stretched to 210 pm and 212 pm (compared to 203 pm without I_{Ti}). The bond elongations and outward relaxation lead to a decrease of the coordination of the surface Ti_{5c} atom, resulting in a more reactive surface site. While weakening the Ti–O bonds to the nearby Ti_{5c} and Ti_{6c} ions in the surface, the I_{Ti} also create new, short bonds to the surrounding lattice oxygens below. They are coordinated by a distorted octahedral environment of lattice oxygens, with Ti–O distances between 189 pm and 206 pm for the first and between 188 pm and 219 pm for the second I_{Ti} type.

The η^2-dioxymethylene is stabilized by 39 kJ mol^{-1} by a subsurface Ti interstitial in the <110> channel exactly below the binding site (Figure 4a); the adsorption energy of −164 kJ mol^{-1} is the most stable binding configuration of formaldehyde on all surfaces considered herein (Table 1). If the I_{Ti} is translated by half a unit cell along the [001] direction into a binding site between two neighboring <110> channels, the effect on the η^2-dioxymethylene structure (Figure 4b) is much smaller ($E_{ads} = -129$ kJ mol^{-1}). The observed stabilization by the defect is a result of a combination of the substantial lattice relaxations around the adsorption site and the correlated decrease the coordination covalent saturation of the surface atoms, which leads to increased adsorption bond strength.

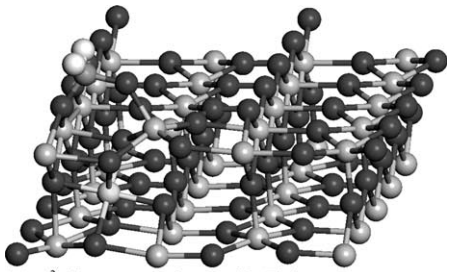

(a) η^2-dioxymethylene with Ti in <110> channel

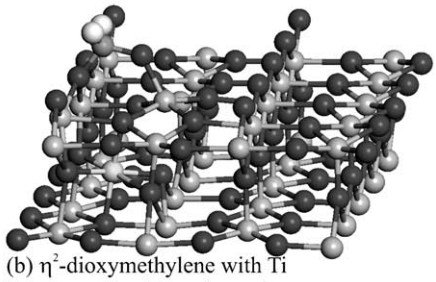

(b) η^2-dioxymethylene with Ti between two <110> channels

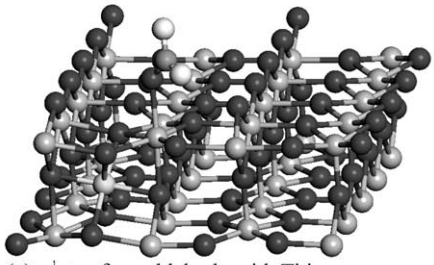

(c) η^1-top formaldehyde with Ti in <110> channel below

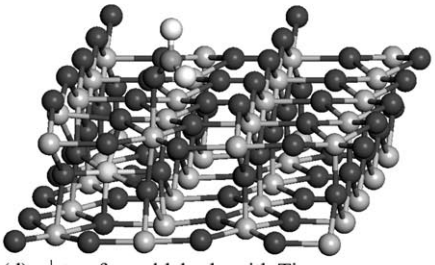

(d) η^1-top formaldehyde with Ti between two <110> channels

Figure 4. Optimized adsorption geometries of formaldehyde on the TiO_2-(110) slab containing an I_{Ti} in a [110] channel site in between the first and second trilayers (a and b, η^2-dioxymethylene structures), and the corresponding structures with the I_{Ti} in between two [110] channels (c and d, η^1-top forms). The I_{Ti} is highlighted in yellow. For clarity only the two uppermost layers of the 5×2 supercells are shown.

Analysis of the projected DOS of formaldehyde in these structures reveals that the bonding is of the same character as it is on the stoichiometric slab and that no different bands (MOs) are formed (Figure 2e–g), but the levels are shifted to lower energy by on average approximately 0.6 eV in the presence of Ti interstitials consistent with a strengthening of the covalent molecule–surface bonds of the η^2 structures. The work functions of the substrate are generally decreased by approximately 0.5 eV to a value of 6.1 eV. To exclude any finite-size effects from the size of the slab in the estimate of the energetic shifts, we performed a calculation with a CH_2O molecule in the middle of the vacuum region between the slabs and found that the presence of Ti interstitials in this case does not affect the MO levels, indicating that the aforementioned downward shift is a real effect in the case of the adsorbed molecule.

The stabilization of the η^2 configurations is linked to strong geometric relaxation of the surface–adsorbate structures, particularly of the Ti_{5c} binding site and the bridging oxygen that bonds to the aldehydic carbon atom. Although the I_{Ti} induce only small length changes to the C–O and the O–Ti bonds of the adsorbate structure (Table 3), they cause an increase in the outward relaxations of the Ti_{5c} site by 28 pm. This leads to larger separations from the subsurface oxygen below. For example, the bonds of the adsorbing Ti_{5c} ions to the lattice O below are stretched to 265 pm in the two η^2-dioxymethylene cases as compared to 183 pm in the oxidized slab and 190 pm when the I_{Ti} is included.

On the opposite site of the six-coordinate Ti ions and the neighboring bridging oxygens, the Ti_{6c} ions are likewise relaxed outward by the adjacent Ti defects as compared to the situation on the stoichiometric slab, but the bond lengths in the lattice below are affected much less (ca. 10 pm) by the I_{Ti}. With the I_{Ti} in the <110> channel, the two Ti_{6c} ions in the bridging row are pushed outward symmetrically by 20 pm, whereas an I_{Ti} in the site between two <110> channels (2nd η^2 configuration) leads to asymmetric relaxations of 58 pm and 16 pm (closer and farther away from I_{Ti}, respectively; this asymmetry can be seen clearly in Figure 4b). The bonds of the Ti_{6c} lattice ion to the bridging oxygens are only slightly perturbed, but the asymmetry due to the I_{Ti} position is found here too (note: $r(Ti_{6c}–O_{br}) = 185$ pm on the clean slab). Clearly, the internal bond lengths are rather insensitive to the amount of stabilization, but the adsorption site changes dramatically.

A harmonic frequency analysis of the normal modes sensitive to the adsorption provides unambiguous evidence for the stabilization (Table 4): While the symmetric and asymmetric ν(O–C–O) stretching modes are only weakly affected by the defects, the molecule surface stretching vibrations ν(Ti_{5c}–O) and the two linear combinations of the involved bridging oxygen to the Ti_{6c} sites show increases of their fre-

Table 4. Harmonic vibrational frequencies in cm^{-1} for η^2-dioxymethylene formaldehyde configurations binding to a Ti_{5c} site and a bridging oxygen on the stoichiometric and subsurface I_{Ti} containing slabs.

Frequencies [cm^{-1}]/ slab	ν_s(O–C–O_{br})	ν_{as}(O–C–O_{br})	ν(Ti_{5c}–O)	ν_{as}(Ti_{6c}–O_{br})	ν_s(Ti_{6c}–O_{br})
stoichiometric	1041	899	599	372	309
I_{Ti} in <110> channel	1046	870	644	440	353
I_{Ti} between two <110> channels	1013	859	640	409	340

quencies by 40 and up to 70 cm^{-1}, respectively. The strongest bonded η^2 structure with the Ti atom in the adjacent <110> channel shows large frequency increases consistent with the stronger molecule–surface interaction.

To elucidate the interaction strength with the surface (E_{int}), we performed a decomposition of the adsorption energies of formaldehyde into the respective elementary components related to surface (E_{surf}) and molecule (E_{mol}) relaxation energies for each configuration.[62] This scheme, though strictly speaking valid only in the absence of electron transfer, allows us to approximate the true bond strength between the molecule and the surface, which is related to the corresponding vibrational frequencies. We expect the charge transfer from the reduced TiO_2 to molecule to be small based on the Mulliken electronegativity of formaldehyde.[12, 63] The interaction energies of the η^2-dioxymethylene configurations in the cases that involve Ti interstitials are calculated at approximately $-570\,kJ\,mol^{-1}$, which is an increase of roughly $40\,kJ\,mol^{-1}$ with respect to stoichiometric TiO_2 and is consistent with the higher frequencies of the ν(Ti–O) stretching modes. The surface relaxation components of the structures with the I_{Ti} in <110> channels and between two such channels are quite large but markedly different, at 206 and $244\,kJ\,mol^{-1}$, which suggests that the asymmetry induced by the defect in the second case results in a higher surface deformation and, hence, a lower adsorption energy. This is consistent with the geometric perturbations from the optimized structure discussed above. Obviously the I_{Ti} enable much larger outward relaxations of the atoms of the binding site in the adsorbate structure with a similar energy cost as in the absence of the defect.

For the stabilization of the η^2 structures, we conclude that the I_{Ti} induce strong changes in the lattice around the adsorption site, which then partially lowers coordination of the Ti_{5c} atom by a weakening of its bonds to the underlying lattice oxygens and leads to stronger molecule–surface interaction. The weakening of bonds of the Ti_{5c} atom to the lattice oxygen corresponds to a decrease of the valence saturation of the adsorption site, which is furthered by the larger outward relaxations in the case of the structures with the subsurface defect. The increased interaction strengths translates into substantially enhanced adsorption in the case of the I_{Ti} in adjacent <110> channels. Electron transfer from the Ti defect, which has been reported for Ti interstitials as well as oxygen vacancies,[40, 47, 50, 51, 53] may contribute to this stabilization, although the insensitivity of the internal bond lengths including the two C–O bonds suggest rather unaffected bond strengths in the molecule and only a minor role for the electron transfer. As mentioned above, we expect the contribution due to electron transfer to be small since the Mulliken electronegativity of formaldehyde is comparably low.[12, 63]

The stabilization of the η^1-top structures by the subsurface I_{Ti}, though similar in nature and also significant, is less pronounced with only up to $21\,kJ\,mol^{-1}$ adsorption energy gain and these structures remain less favorable than the η^2-dioxymethylene configurations. With an interstitial in the <110> channel adjacent to the Ti_{5c} binding site (type I; Figure 4c), an adsorption energy of $-90\,kJ\,mol^{-1}$ is obtained, whereas an I_{Ti} between two neighboring <110> channels (type II; Figure 4d) is less effective in stabilizing the adsorbate ($E_{ads} = -82\,kJ\,mol^{-1}$).

Comparison of the projected DOS features for the η^1-top structures (Figure 2b–d) on the different slabs with and without Ti interstitials points to a consistently unchanged bonding mechanism and no formation of different covalent bonds. This is supported by structural features of the adsorbed molecules, which in the presence of the I_{Ti} only differ slightly from those on the stoichiometric slab. The C=O bond length remains unchanged at 123 pm (Table 2) despite the presence of the I_{Ti} below, and is not very sensitive to the stabilization. The harmonic frequency analysis (Table 2), on the other hand, reveals a low-frequency shift of 40–50 cm^{-1} of the ν(C=O) vibration in the presence of the I_{Ti}, indicating a weakening of the C=O double bond by the stabilization. This is likely due to a small charge transfer from the Ti_{5c} site into the antibonding $2\pi^*$ level of the adsorbed molecule.

The Ti_{5c}–O adsorption bond is shortened by the defects more evidently by approximately 10 pm to 213–216 pm, which correlates with a slight frequency increase of the ν(Ti_{5c}–O) stretching modes by approximately 20 cm^{-1} (Table 2) and an increase of the interaction energies by 25–30 $kJ\,mol^{-1}$ (Table 5). The Ti_{5c} ion itself is moved outward slightly farther with 16 pm from its relaxed position without

Table 5. Energy decomposition of the adsorption energies of formaldehyde on stoichiometric and defective TiO_2 surfaces at a coverage of 0.1 ML. E_{ads}, E_{surf}, E_{mol}, and E_{int} are the adsorption energy, surface, and molecule relaxation energy, and total interaction energy, respectively.

Energies [$kJ\,mol^{-1}$]/ slab	E_{ads}	E_{surf}	E_{mol}	E_{int}
η^1-top:				
stoichiometric	−69	21	1	−91
sub-T_{i5c} V_O	−135	19	10	−164
I_{Ti} in <110> channel	−90	27	2	−119
I_{Ti} between two <110> channels	−82	29	3	−114
η^2-dioxymethylene:				
stoichiometric	−125	219	189	−534
I_{Ti} in <110> channel	−164	206	204	−574
I_{Ti} between two <110> channels	−129	244	199	−572

adsorbate, stretching the bond to the lattice oxygen below. This causes slightly increased surface relaxation energies by 27–29 kJ mol^{-1}.

The stabilization effect of the subsurface interstitials is quite short-ranged and a translation of the I_{Ti} by a unit cell along the row [001] direction away from formaldehyde recovers the binding energies to within 5 kJ mol^{-1} of the value on the stoichiometric surface. For the η^1-top configurations, displacing the I_{Ti} to a deeper site between the second and third trilayer likewise reduces the adsorption energies to values close to the reference on the stoichiometric TiO_2 slab. However, since computational limitations force us to use only a four trilayer slab with the third and fourth layers frozen, the geometry relaxation around the I_{Ti} is incomplete and, hence, the resulting effect represents a lower bound for the stabilization.

III. Bonding to defective surfaces with oxygen vacancies: Surface and subsurface oxygen vacancies ("V_O") lead to comparable stabilization of the formaldehyde bonding, but the resulting adsorption energies remain substantially lower than those obtained in the presence of subsurface interstitials. Before we present the results, we discuss briefly the formation energy of the four types of possible V_O in the near-surface region: surface bridging and in-plane oxygen vacancies, and subsurface vacancies below five-coordinate Ti sites and below the bridging oxygen row, both of which become equivalent by symmetry in the bulk.

Of the two subsurface oxygen defects, the calculated formation energy of a sub-Ti_{5c} vacancy right below the first layer is 520 kJ mol^{-1} (using as a reservoir the O atoms in O_2 gas). This value exceeds the experimental bulk vacancy formation energy of 439 kJ mol^{-1},[64] whereas the formation of a sub-bridging oxygen row vacancy is energetically less costly (323 kJ mol^{-1}) and more favorable than that of a surface in-plane oxygen vacancy (378 kJ mol^{-1}).[65] The formation energies of surface-bridging oxygen vacancies are considerably lower, 272 kJ mol^{-1} at 0.1 ML coverage, but depend strongly on the concentration and rise to 282 and 331 kJ mol^{-1} in 3×2 and 2×2 supercells, which correspond to coverages of 0.16 and 0.25 ML, respectively. The formation energies of the subsurface oxygen vacancies show a similar increase to 526 and 345 kJ mol^{-1} in a 3×2 supercell.

Since GGA functionals are known to overbind O_2 in the gas phase (ca. 92 kJ mol^{-1} for PW91),[66] the reported defect formation energies in the literature are usually underestimated unless corrected. A correction of the overbinding would increase the formation energies by a constant value, but not their order, so for the following discussion we only present the uncorrected results. Our estimated vacancy formation energies are generally in line with earlier results, which reported values of 340 kJ mol^{-1} (GGA-PBE functional, 0.25 ML coverage, triplet state),[19] 355 kJ mol^{-1} (PBE+U functional, 0.25 ML coverage),[50] and 366 kJ mol^{-1} (PW91 functional, 0.25 ML coverage)[38] for bridging oxygen vacancies, and somewhat lower than previous LDA results.[39] Bulk oxygen vacancy formation energies have been reported in the literature with a considerable spread, with values as low as 431 kJ mol^{-1} (PW91 functional, 1 V_O per 54 atom supercell)[10] to 543 kJ mol^{-1} (PBE functional, 1 V_O per 54 atom supercell).[19] Interestingly, the authors of the aforementioned study also obtained a value of 491 kJ mol^{-1} (PW1PW functional, 1 V_O per 54 atom supercell) using a hybrid functional, which suggests the vacancy concentrations implied by the size of the supercell is more important in determining accurate formation energies than the choice of the exchange-correlation functional and may explain the spread of values in the literature.

The adsorption of formaldehyde in a bridging oxygen vacancy (Figure 5a) is enhanced by 17 kJ mol^{-1} to a value of -86 kJ mol^{-1} (Table 1) as compared to the η^1-top configuration on a stoichiometric slab. In the optimized geometry, the molecular plane is oriented parallel to the bridging oxygen rows and the symmetrically identical $r(Ti_{6c}–O_{ald})$ distances in the former vacancy site are elongated to 230 pm. The calculated aldehydic C=O bond length is 124 pm, suggesting that the double-bond character is mostly intact and the adsorption perturbs the molecule only weakly. Compared to the η^2-dioxymethylene structure, the Ti–O bond lengths on the bridging oxygen site are elongated and the binding energy is lower by approximately 40 kJ mol^{-1}.

Since this configuration is clearly less stable than the η^2-dioxymethylene structure on the stoichiometric surface, bonding in a bridging oxygen vacancy is clearly unfavorable. This is in contrast to experimental studies, which suggest

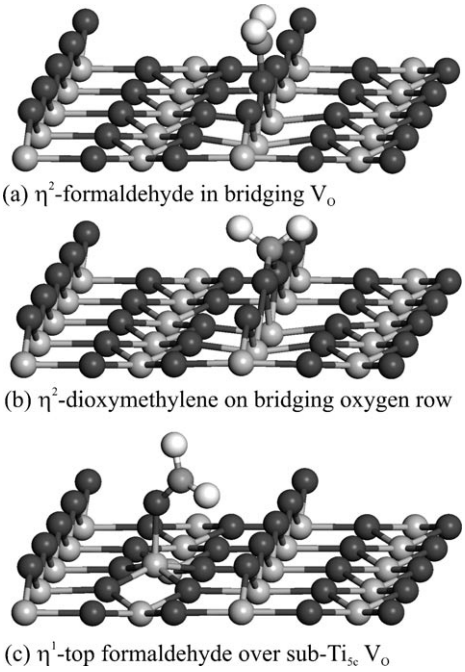

Figure 5. Optimized adsorption geometries of formaldehyde binding in the presence of a surface containing a bridging (a and b) or a subsurface V_O defect below a formerly five-coordinate Ti site c). The subsurface V_O is below the Ti surface atom that is at a higher position than other Ti atoms and to which the formaldehyde is bonded.

that adsorption in bridging oxygen vacancies should be favored and would lead to a coupling pathway to olefins, thus healing the vacancies.[55] However, recent experimental results from our own work on acrolein and benzaldehyde are in contrast to those earlier findings and show that the point defects driving the reaction are bulk interstitials.[57, 60]

The slight stabilization of the adsorption by the bridging oxygen vacancy is due to the formation of a new, covalently bonded configuration (as evidenced by the distances $r(Ti_{6c}–O_{ald})$), which is very different from the η^1 and η^2 structures of the stoichiometric surface. Hence the stabilization is a direct consequence of the changed electronic bonding situation of the new adsorption site, in which the excess electrons from the defect,[12, 47, 50] which correlate with the loss of coordination of the Ti_{6c} atoms, participate in the formation of the covalent bonds.

Furthermore, our calculations identified a second stable configuration of formaldehyde on a V_O, which resembles another η^2-dioxymethylene intermediate (Figure 5b) that occurs during the diffusion process of vacancy-bonded formaldehyde along a bridging oxygen row. This configuration has a binding energy of $-95\,kJ\,mol^{-1}$ (Table 1), slightly more stable than the simple vacancy adsorption. The methylene group is rotated by 90° with respect to the rows and binds to two bridging oxygen atoms in this structure, but both sides are slightly asymmetric with the CH_2 unit being closer to one lattice O ($r(C–O) = 140$ pm, vs. 144 pm to the other bridging oxygen). The asymmetry is reflected in the $O–Ti_{6c}$ distances, which on the closer side are elongated to 194 and 214 pm to the outer and central Ti ions, respectively. On the longer side, the bridging oxygen is detached from its outer Ti_{6c} neighbor ($r(O–Ti_{6c}) = 291$ pm), whereas the distance to the center Ti_{6c} is 192 pm. Compared to the distance on the clean surface (185 pm), all the $Ti_{6c}–O$ bonds are significantly stretched and point to a strong covalent bond of the new "bridging oxygen" to the CH_2 fragment, giving it a dioxymethylene character rather than an isolated "carbene".

The effective range of significant stabilization by a bridging V_O is very narrow, similar to the case of the Ti interstitials, and indicates that again the lack of valence saturation of the adsorption site (caused here by the loss of bond neighbors) is crucial for the effect: The binding energy in the in η^1-top structure on a five-coordinate Ti ion adjacent to the vacancy is $-66\,kJ\,mol^{-1}$ and the geometry of this diagonal formaldehyde configuration is essentially unaffected. Although this is different than the adsorption behavior reported for O_2,[12] it is reasonable since the charge transfer from the defect to molecule is much smaller in the case of formaldehyde as estimated from its electronegativity.[12, 63]

Moreover, in-plane oxygen vacancies can be conceived on the TiO_2(110) surface and, in some cases, they could stabilize adsorption slightly less than bridging oxygen vacancies. Since to our knowledge such V_O have not been identified on TiO_2(110), they appear to be unimportant under experimental conditions and will only be discussed briefly. Unlike bridging oxygen vacancies, in-plane oxygen vacancies do not truly stabilize adsorption on adjacent Ti_{5c} ions, but in every tested configuration we find that formaldehyde heals the defect by moving with its oxygen into the V_O during the optimization. A set of different structures resulted in which a methylene group was bonded to the new in-plane oxygen, and either an adjacent bridging oxygen ($E_{ads} = -79\,kJ\,mol^{-1}$), or a neighboring Ti_{5c} ion ($E_{ads} = -33\,kJ\,mol^{-1}$). In both cases singlet ground states are obtained and $O_{ip}–C$ bond lengths of 148 and 144 pm, respectively, implying that the character of the aldehydic bond is reduced to a single bond. The $O_{br}–C$ bond length of 139 pm in the first configuration (O_{br}-CH_2-O_{ip}) also suggests single-bond character. The Ti–C bond of the second configuration is 210 pm, close to distances found for Ti^{IV}–compounds.[67]

In contrast, subsurface oxygen vacancies lead to a much more substantial stabilization of the binding than surface V_O. Of the two types of subsurface oxygen vacancies, only vacancies right below the Ti_{5c} ("sub-Ti_{5c}") binding formaldehyde in an η^1-top configuration lead to a significant stabilization of approximately $66\,kJ\,mol^{-1}$ ($E_{ads} = -135\,kJ\,mol^{-1}$ for the diagonal η^1 orientation; Figure 5c). Geometrically, adsorption above the sub-Ti_{5c} oxygen vacancy leads to a large outward relaxation of the five-coordinate Ti ion by 77 pm (Table 2). The strong adsorption correlates with a much larger interaction energy of $-164\,kJ\,mol^{-1}$ (compared to $-91\,kJ\,mol^{-1}$ on stoichiometric TiO_2) and a shortened bond from the aldehydic oxygen to the Ti_{5c} ($r(Ti_{5c}–O) = 196$ pm).

With an adsorption energy of $-135\,kJ\,mol^{-1}$, these η^1-top configurations above oxygen vacancies below the Ti_{5c} could compete with the η^2-dioxymethylene configuration on defect free regions of the surface. However, the formation energies of such subsurface V_O are very high compared to surface bridging oxygen vacancies, and therefore subsurface V_O defects are quite unfavorable, probably playing only a minor role. EPR studies by Jenkins and Murphy[30] as well as molecular dynamics simulations by Jug et al.[68] provide evidence against the presence of subsurface (and bulk) oxygen vacancies since their migration to the surface at conditions used typically for cleaning of titania is a rather facile process.[68] In fact, the η^1 configurations on top of sub-Ti_{5c} vacancies are $207\,kJ\,mol^{-1}$ higher in total energy than the structure of the η^2-dioxymethylene binding in a surface bridging oxygen vacancy, which reflects the unfavorable formation cost of subsurface V_O.

By analogy to the behavior of surface oxygen vacancies, the effects of subsurface oxygen vacancies decay quickly with the distance form the binding site. A translation of the sub-Ti_{5c} oxygen vacancy by one unit cell along the [001] direction away from the formaldehyde binding site leads to essentially unperturbed adsorption energies ($-70\,kJ\,mol^{-1}$ for the diagonal η^1-top configuration). Also, an oxygen vacancy below the bridging oxygen row adjacent to a Ti_{5c} binding site is already too far away, and leads to an adsorption energy of $-63\,kJ\,mol^{-1}$ for the η^1-top configuration. We performed a limited set of computations on the variation of the stabilization with vertical distance and found that formaldehyde adsorption is little affected by oxygen vacancies below

the second layer. Using the four-trilayer slab, we removed an oxygen atom in between the second and third trilayers below a Ti_{5c} binding site and optimized the adsorption η^1 structure on top, while keeping the bottom layers frozen. In this case the adsorption energy of formaldehyde varied only slightly ($-71\,kJ\,mol^{-1}$) from the value obtained for the corresponding diagonal η^1-top configuration on the stoichiometric slab.

In summary, we find that all defects exert significantly different, characteristic stabilization effects on the formaldehyde adsorption depending on the binding structure, and induce it to assume different surface configurations. This, in turn, influences the chemical character of the different surface species. The presence of subsurface interstitials leads to the most favorable adsorption energies, followed by subsurface oxygen vacancies and surface bridging oxygen vacancies. Generally the covalently bonded η^2-dioxymethylene-type structures involving bridging oxygens are significantly more stable than η^1-top configurations in all cases considered. Such structures are likely to dominate the adsorption on oxidized and reduced rutile TiO_2(110) surfaces.

Conclusion

We report the first systematic investigation of the effects of different surface and subsurface point defects on the adsorption of formaldehyde as a probe for carbonyls on rutile TiO_2(110) surfaces using first-principles DFT calculations.

The most stable adsorption structure of formaldehyde at low coverages of 0.1 ML is η^2-dioxymethylene with a second C–O bond stretching to a nearby bridging oxygen atom ($E_{ads} = -125\,kJ\,mol^{-1}$). Though still strongly bonded, the η^1-top configuration bonding in electrostatic fashion with an oxygen lone pair to a five-coordinate Ti^{4+} site is clearly less favorable ($E_{ads} = -69\,kJ\,mol^{-1}$).

Point defects such as surface bridging oxygen vacancies, titanium interstitials, and subsurface oxygen vacancies stabilize the adsorption significantly. The stabilization is due to a combination of lattice changes due to the presence of the defects, which result in partial loss of coordination of the surface atoms, particularly at the Ti_{5c} sites, and lead to stronger molecule–surface interactions. The I_{Ti} induce a weakening of the bonds between the Ti_{5c} atoms and the lattice oxygen underneath, while itself creating new bonds with these lattice oxygen. Additionally, the presence of a subsurface defect leads to a substantial increase of the outward relaxation that further enhances the adsorption bonding through a stronger interaction energy.

Subsurface Ti interstitials between the first and second layer exert a strong stabilization on the adsorption. Ti interstitials in a <110> channel near a five-coordinate Ti site stabilize the η^2-dioxymethylene structures by as much as $95\,kJ\,mol^{-1}$ ($E_{ads} = -164\,kJ\,mol^{-1}$). The adsorption of formaldehyde in a bridging oxygen vacancy leads to an η^2-dioxymethylene ($E_{ads} = -95\,kJ\,mol^{-1}$) structure between two bridging oxygens, which is slightly more stable than η^2-formaldehyde ($E_{ads} = -86\,kJ\,mol^{-1}$) in a single vacancy. The largest stabilization is found for a subsurface oxygen vacancy below a five-coordinate Ti site, which favors the η^1-top adsorption of formaldehyde by $-66\,kJ\,mol^{-1}$ ($E_{ads} = -135\,kJ\,mol^{-1}$). However, the η^2-dioxymethylene structures stabilized by interstitials represent the most strongly bonded species.

From these results we conclude that the preferred adsorption structure of formaldehyde on a stoichiometric surface, in the presence of small concentrations of subsurface Ti interstitials or surface oxygen vacancies, is an η^2-dioxymethylene configuration with involvement of a five-coordinate Ti ion. Clearly, for all tested surface defects we find substantial stabilization of the adsorption energies, which indicates that reaction intermediates and activation barriers will be affected strongly by the presence of defects. Thus, even if the point defects remain static and do not participate directly in surface reactions, they may lead to major changes in the surface reactivity. It is, therefore, essential to consider all the types of point defects at realistic concentrations in investigations on TiO_2 and other reducible oxides to obtain correct adsorption sites, structures, energetic, and chemiphysical properties, and to successfully connect to experiments performed on reduced titania samples, as employed in UHV model studies.

Computational Details

All calculations in the present study have been carried out using the Vienna Ab-Initio Simulation Package (VASP).[69, 70] The Generalized-Gradient-Approximation functional PW91[71] was employed together with the Projector-Augmented Wavefunction method.[72] Despite the fact that GGA functionals underestimate the band-gap by as much as approximately 30% and fail to reproduce the band gap states caused by point defects,[4, 5, 10, 26, 73, 74] we have chosen this functional since it has been shown to give very reliable energetics and structures on titania. The theoretical results, for instance, for oxygen vacancy formation[4, 10, 19, 26, 73, 74] or dissociative H_2O adsorption[18, 25, 74] match experimental data well. The unoccupied states of a band gap are excited states and, thus, require the use of time-dependent DFT or other excited-state methods such as complete active space or configuration interaction theories for a physically correct treatment. Although time-independent DFT employing hybrid exchange-correlation functionals such as B3LYP,[75] PW1PW[76] or PBE0,[77] is often used to reproduce the gap states and spin-polarized ground states of oxygen vacancies and interstitials, these functionals lead to an asymmetry in the lattice relaxation caused by oxygen vacancies.[78] However, no significant asymmetry around bridging oxygen vacancies has been observed in STM thus far.[11, 15, 26, 40, 43, 44, 79, 80] Accordingly, we have restricted our studies to calculations using a GGA functional since we are primarily interested in energetic and geometric details of the adsorption of a probe molecule on the defective TiO_2(110) surfaces.

We use a plane-wave basis set with a kinetic cut-off energy of 400 eV and Gaussian smearing ($\sigma = 0.2$ eV) to determine electronic occupancies. The structural model that represents the surface consists of a four trilayer slab of TiO_2(110) terminated on both sides by bridging oxygen rows, separated by vacuum (ca. 15 Å) from its periodic images, using interatomic distances from the optimized bulk rutile unit cell. We considered several different supercell sizes including 2×2, 3×2, and 5×2 supercells of the ideal surface cell to estimate the magnitude of lateral interactions. Corresponding Γ-centered $3\times3\times1$, $2\times3\times1$, and $1\times3\times1$ Monkhorst-Pack k-point meshes[81] were used for integrations in reciprocal space. For the

sake of simplicity, we will focus in this article on the low coverage represented by the 5×2 supercell with one adsorbed formaldehyde molecule, corresponding to a theoretical coverage of 0.1 monolayer.

Formaldehyde was placed in initial structures on one side of the slab and optimizations were carried out relaxing all degrees of freedom of the molecule, and the two uppermost trilayers. Thresholds of 10^{-5} eV were used for electronic, and 0.01 eV Å^{-1} for force convergence. Dipole corrections were employed along the vacuum direction of the supercell.[82] Oxygen vacancies were modeled by removing atoms from the slab, and interstitials by placing Ti atoms at appropriate sites. The dependence of the energies on the lateral distance between defects and the molecules was tested in all cases, and a rough estimate for the effect of vertical separation was obtained by placing vacancies or interstitials in between the second and third layers below the surface.

Adsorption energies are calculated as the relative energy difference between an optimized molecule–surface complex and the respective relaxed clean surface and gas-phase molecule. The convergence of the adsorption energies reported here has been carefully tested by increasing the plane-wave cutoff (up to 600 eV), the k-points meshes (up to $3\times5\times1$), the smearing parameter (0.15 to 0.3 eV) and the slab thickness (5 trilayers). Our relative energies and structures are well-converged to within 5 kJ mol^{-1}. All obtained local minima were characterized by a harmonic vibrational analysis at the Γ point, by calculating the frequencies of the adsorbate vibrations (including the atoms of the first TiO_2 trilayer) from diagonalization of the Hessian matrices. The Hessians have been computed by numerical second derivation of the total energy with respect to the Cartesian coordinates (displacements of ±0.025 Å were found to give converged frequencies). Since the mass of Ti is only about three times heavier than O, strong coupling between energetically close molecular modes and phonons spreads the molecule surface vibrations out into various normal modes at close frequencies. For the sake of simplicity, we only report the frequencies that correspond to linear combinations of atomic motion which have dominant contributions of the vibrations of interest.

Spin-polarization was tested in all cases, but we will only report spin-polarization for the few cases in which a non-singlet ground state was found. We caution the reader that GGA functionals generally find the singlet states at similar or slightly lower total energies as the triplet states, thus usually not correctly reproducing the spin-polarized character of point defects.[4, 5, 10, 38, 50] The error induced by this shortcoming, for instance, in the oxygen vacancy formation energy, is much smaller than the change in energy due to higher coverages/densities compared to typical vacancy concentrations (smaller supercells)[18, 38, 39] or the well-known overbinding of O_2 by GGA functionals.[66]

Acknowledgements

The authors gratefully acknowledge support of this work by the Harvard NSEC supported by the National Science Foundation under award, NSF/PHY 06-46094. J.H. acknowledges support through a Feodor-Lynen fellowship of the A. v. Humboldt foundation.

[1] U. Diebold, *Surf. Sci. Rep.* **2003**, *48*, 53.
[2] C. Lun Pang, R. Lindsay, G. Thornton, *Chem. Soc. Rev.* **2008**, *37*, 2328.
[3] T. L. Thompson, J. T. Yates, *Chem. Rev.* **2006**, *106*, 4428.
[4] M. V. Ganduglia-Pirovano, A. Hofmann, J. Sauer, *Surf. Sci. Rep.* **2007**, *62*, 219.
[5] G. Pacchioni, *J. Chem. Phys.* **2008**, *128*, 182505.
[6] A. Linsebigler, G. Q. Lu, J. T. Yates, *J. Chem. Phys.* **1995**, *103*, 9438.
[7] J. Nowotny, T. Bak, M. K. Nowotny, L. R. Sheppard, *Int. J. Hydrogen Energy* **2007**, *32*, 2609.
[8] T. Bak, J. Nowotny, M. K. Nowotny, *J. Phys. Chem. B* **2006**, *110*, 21560.
[9] M. Li, W. Hebenstreit, U. Diebold, A. M. Tyryshkin, M. K. Bowman, G. G. Dunham, M. A. Henderson, *J. Phys. Chem. B* **2000**, *104*, 4944.
[10] M. M. Islam, T. Bredow, A. Gerson, *Phys. Rev. B* **2007**, *76*, 045217.
[11] S. Wendt, P. T. Sprunger, E. Lira, G. K. H. Madsen, Z. S. Li, J. O. Hansen, J. Matthiesen, A. Blekinge-Rasmussen, E. Laegsgaard, B. Hammer, F. Besenbacher, *Science* **2008**, *320*, 1755.
[12] N. A. Deskins, R. Rousseau, M. Dupuis, *J. Phys. Chem. C* **2010**, *114*, 5891.
[13] P. Stone, R. A. Bennett, M. Bowker, *New J. Phys.* **1999**, *1*, 8.
[14] M. A. Henderson, W. S. Epling, C. L. Perkins, C. H. F. Peden, U. Diebold, *J. Phys. Chem. B* **1999**, *103*, 5328.
[15] U. Diebold, J. Lehman, T. Mahmoud, M. Kuhn, G. Leonardelli, W. Hebenstreit, M. Schmid, P. Varga, *Surf. Sci.* **1998**, *411*, 137.
[16] W. S. Epling, C. H. F. Peden, M. A. Henderson, U. Diebold, *Surf. Sci.* **1998**, *412–413*, 333.
[17] L. Q. Wang, D. R. Baer, M. H. Engelhard, *Surf. Sci.* **1994**, *320*, 295.
[18] M. D. Rasmussen, L. M. Molina, B. Hammer, *J. Chem. Phys.* **2004**, *120*, 988.
[19] X. Y. Wu, A. Selloni, M. Lazzeri, S. K. Nayak, *Phys. Rev. B* **2003**, *68*, 241402.
[20] E. Farfan-Arribas, R. J. Madix, *Surf. Sci.* **2003**, *544*, 241.
[21] J. Oviedo, R. Sanchez-De-Armas, M. A. S. Miguel, J. F. Sanz, *J. Phys. Chem. C* **2008**, *112*, 17737.
[22] Z. R. Zhang, O. Bondarchuk, J. M. White, B. D. Kay, Z. Dohnalek, *J. Am. Chem. Soc.* **2006**, *128*, 4198.
[23] M. A. Henderson, *Surf. Sci.* **1996**, *355*, 151.
[24] G. Lu, A. Linsebigler, J. T. Yates, *J. Phys. Chem.* **1994**, *98*, 11733.
[25] H. Perron, J. Vandenborre, C. Domain, R. Drot, J. Roques, E. Simoni, J. J. Ehrhardt, H. Catalette, *Surf. Sci.* **2007**, *601*, 518.
[26] T. Minato, Y. Sainoo, Y. Kim, H. S. Kato, K. Aika, M. Kawai, J. Zhao, H. Petek, T. Huang, W. He, B. Wang, Z. Wang, Y. Zhao, J. L. Yang, J. G. Hou, *J. Chem. Phys.* **2009**, *130*, 124502.
[27] T. J. Gray, C. C. McCain, N. G. Masse, *J. Phys. Chem.* **1959**, *63*, 472.
[28] V. E. Henrich, R. L. Kurtz, *Phys. Rev. B* **1981**, *23*, 6280.
[29] M. A. Henderson, *Surf. Sci.* **1999**, *419*, 174.
[30] C. A. Jenkins, D. M. Murphy, *J. Phys. Chem. B* **1999**, *103*, 1019.
[31] M. Aono, R. R. Hasiguti, *Phys. Rev. B* **1993**, *48*, 12406.
[32] G. Mattioli, F. Filippone, P. Alippi, A. A. Bonapasta, *Phys. Rev. B* **2008**, *78*, 241201.
[33] A. K. Ghosh, F. G. Wakim, R. R. Addiss, *Phys. Rev.* **1969**, *184*, 979.
[34] F. Millot, M. G. Blanchin, R. Tetot, J. F. Marucco, B. Poumellec, C. Picard, B. Touzelin, *Prog. Solid State Chem.* **1987**, *17*, 263.
[35] D. C. Cronemeyer, *Phys. Rev.* **1959**, *113*, 1222.
[36] P. J. D. Lindan, N. M. Harrison, M. J. Gillan, J. A. White, *Phys. Rev. B* **1997**, *55*, 15919.
[37] A. Bouzoubaa, A. Markovits, M. Calatayud, C. Minot, *Surf. Sci.* **2005**, *583*, 107.
[38] J. Oviedo, M. A. San Miguel, J. F. Sanz, *J. Chem. Phys.* **2004**, *121*, 7427.
[39] K. Hameeuw, G. Cantele, D. Ninno, F. Trani, G. Iadonisi, *Phys. Status Solidi A* **2006**, *203*, 2219.
[40] Y. Sakai, S. Ehara, *Jpn. J. Appl. Phys.* **2001**, *40*, L773.
[41] W. Göpel, J. A. Anderson, D. Frankel, M. Jaehnig, K. Phillips, J. A. Schafer, G. Rocker, *Surf. Sci.* **1984**, *139*, 333.
[42] M. A. Henderson, *Surf. Sci.* **1995**, *343*, L1156.
[43] Z. Zhang, Y. Du, N. G. Petrik, G. A. Kimmel, I. Lyubinetsky, Z. Dohnalek, *J. Phys. Chem. C* **2009**, *113*, 1908.
[44] X. F. Cui, B. Wang, Z. Wang, T. Huang, Y. Zhao, J. L. Yang, J. G. Hou, *J. Chem. Phys.* **2008**, *129*, 044703.
[45] C. L. Perkins, M. A. Henderson, *J. Phys. Chem. B* **2001**, *105*, 3856.
[46] G. Rocker, J. A. Schaefer, W. Gopel, *Phys. Rev. B* **1984**, *30*, 3704.
[47] T. Bredow, G. Pacchioni, *Chem. Phys. Lett.* **2002**, *355*, 417.
[48] C. Di Valentin, *J. Chem. Phys.* **2007**, *127*, 154705.
[49] N. A. Deskins, *Chem. Phys. Lett.* **2009**, *471*, 75.
[50] B. J. Morgan, G. W. Watson, *J. Phys. Chem. C* **2009**, *113*, 7322.
[51] P. Krüger, S. Bourgeois, B. Domenichini, H. Magnan, D. Chandesris, P. Le Fevre, A. M. Flank, J. Jupille, L. Floreano, A. Cossaro, A. Verdini, A. Morgante, *Phys. Rev. Lett.* **2008**, *100*, 055501.

[52] C. Di Valentin, G. Pacchioni, A. Selloni, *J. Phys. Chem. C* **2009**, *113*, 20543.
[53] E. Finazzi, C. Di Valentin, G. Pacchioni, *J. Phys. Chem. C* **2009**, *113*, 3382.
[54] M. A. Henderson, *J. Phys. Chem. B* **2004**, *108*, 18932.
[55] H. Qiu, H. Idriss, Y. M. Wang, C. Woell, *J. Phys. Chem. C* **2008**, *112*, 9828.
[56] H. Idriss, K. S. Kim, M. A. Barteau, *Surf. Sci.* **1992**, *262*, 113.
[57] L. Benz, J. Haubrich, R. G. Quiller, C. M. Friend, *Surf. Sci.* **2009**, *603*, 1010.
[58] M. A. Henderson, *Langmuir* **2005**, *21*, 3443.
[59] R. T. Zehr, M. A. Henderson, *Surf. Sci.* **2008**, *602*, 2238.
[60] L. Benz, J. Haubrich, R. G. Quiller, S. C. Jensen, C. M. Friend, *J. Am. Chem. Soc.* **2009**, *131*, 15026 – 15031.
[61] On the clean slab, the optimized Ti−O distances are 185 pm and 196 pm to the bridging (from six-coordinate Ti, $r(Ti_{6c}–O_{br})$) and in-plane oxygens ($r(Ti_{5c}–O_{ip})$), respectively.
[62] J. Haubrich, D. Loffreda, F. Delbecq, P. Sautet, Y. Jugnet, C. Becker, K. Wandelt, *J. Phys. Chem. C* **2010**, *114*, 1073.
[63] R. G. Pearson, *Inorg. Chem.* **1988**, *27*, 734.
[64] P. Kofstad, *Nonstoichiometry, Diffusion, and Electrical Conductivity in Binary Metal Oxides*, Wiley, New York, **1972**, Chapter 8.
[65] The energies of the vacancies in a spin-polarized triplet state have been obtained at very similar, though marginally higher values compared to the non-spin polarized solutions. Hence the formation energy estimates are given only for the singlet states. This problem of GGA functionals has already been discussed in reference [38].
[66] J. P. Perdew, K. Burke, M. Ernzerhof, *Phys. Rev. Lett.* **1996**, *77*, 3865.
[67] M. Basso-Bert, P. Cassoux, F. Crasnier, D. Gervais, J.-F. Labarre, P. De Loth, *J. Organomet. Chem.* **1977**, *136*, 201.
[68] K. Jug, N. N. Nair, T. Bredow, *Phys. Chem. Chem. Phys.* **2005**, *7*, 2616.
[69] G. Kresse, J. Hafner, *Phys. Rev. B* **1993**, *47*, 558.
[70] G. Kresse, J. Hafner, *Phys. Rev. B* **1993**, *48*, 13115.
[71] J. P. Perdew, Y. Wang, *Phys. Rev. B* **1992**, *45*, 13244.
[72] G. Kresse, D. Joubert, *Phys. Rev. B* **1999**, *59*, 1758.
[73] E. Finazzi, C. Di Valentin, G. Pacchioni, A. Selloni, *J. Chem. Phys.* **2008**, *129*, 154113.
[74] P. M. Kowalski, B. Meyer, D. Marx, *Phys. Rev. B* **2009**, *79*, 115410.
[75] A. D. Becke, *J. Chem. Phys.* **1993**, *98*, 5648.
[76] T. Bredow, A. R. Gerson, *Phys. Rev. B* **2000**, *61*, 5194.
[77] C. Adamo, V. Barone, *J. Chem. Phys.* **1999**, *110*, 6158.
[78] C. Di Valentin, G. Pacchioni, A. Selloni, *Phys. Rev. Lett.* **2006**, *97*, 166803.
[79] U. Diebold, W. Hebenstreit, G. Leonardelli, M. Schmid, P. Varga, *Phys. Rev. Lett.* **1998**, *81*, 405.
[80] G. H. Enevoldsen, H. P. Pinto, A. S. Foster, M. C. R. Jensen, A. Kuhnle, M. Reichling, W. A. Hofer, J. V. Lauritsen, F. Besenbacher, *Phys. Rev. B* **2008**, *78*, 045416.
[81] H. J. Monkhorst, J. D. Pack, *Phys. Rev. B* **1976**, *13*, 5188.
[82] J. Neugebauer, M. Scheffler, *Phys. Rev. B* **1992**, *46*, 16067.

Received: September 7, 2010
Published online: March 23, 2011

